Miner Deposita (2015) 50:795–809
DOI 10.1007/s00126-014-0575-7

ARTICLE

Geochemistry of magnetite from Proterozoic Fe-Cu deposits in the Kangdian metallogenic province, SW China

Wei Terry Chen · Mei-Fu Zhou · Jian-Feng Gao · Ruizhong Hu

Received: 22 May 2014 / Accepted: 29 December 2014 / Published online: 18 January 2015

Abstract Fe-Cu deposits in the Kangdian Fe-Cu metallogenic province, SW China, are hosted in Paleoproterozoic meta-volcanic-sedimentary sequences and are spatially associated with coeval mafic intrusions. Several well-known examples are the giant Lala, Dahongshan, and Yinachang deposits. They have a common paragenetic sequence of an early Fe-oxide stage associated with sodic alteration and a late Cu-sulfide stage associated with potassic-carbonate alteration. Magnetite dominates the Fe-oxide stage of these deposits but is also present in the Cu-sulfide stage of the Lala deposit. This study uses trace element compositions of magnetite to examine the nature and origin of the ore-forming fluids. The magnetite has variable concentrations of Ti, Al, Mg, Mn, Si, V, Cr, Ca, Co, Ni, Sc, Zn, Cu, Mo, Sn, and Ga, which are thought to have been controlled mainly by fluid compositions and/or intensive parameters (e.g., temperature and oxygen fugacity (fO_2)). Fluid-rock interaction and coprecipitating mineral phases appear to be less important in controlling the magnetite compositions. Magnetite grains in the Fe-oxide stage of the Lala and Dahongshan deposits have comparable trace element compositions and were likely precipitated from chemically similar fluids. High Ni contents of magnetite in both deposits, coupled with previous isotopic data and the fact that the two deposits are spatially associated with coeval mafic intrusions, strongly suggest that the ore-forming fluids were genetically related to the mafic magmas that formed the intrusions. Magnetite grains in the Fe-oxide stage of the Yinachang deposit have much lower V and Ni but higher Sn and Mo contents than those of the Lala and Dahongshan deposits and are thus thought to have precipitated from more oxidized and Mo-Sn-rich fluids that may have evolved from relatively felsic magmas. Magnetite grains from the Cu-sulfide and Fe-oxide stages of the Lala deposit are broadly similar in composition, but those in the Cu-sulfide stage have slightly higher Cu, Zn, and Mn and are thought to have crystallized from relatively low-temperature and Cu-Zn-Mn-rich fluids evolved from the fluids of the early Fe-oxide stage. Our results show that magnetite from the Fe-Cu deposits in the Kangdian Province, banded iron formation, Fe skarn deposits, diabase-hosted hydrothermal Fe deposits, and magmatic deposits has significantly different compositions. We propose that covariations of Co-Ni, Zn-Sn, and Co/Ni-Mn can be used to effectively discriminate different deposit types.

Keywords Magnetite · Trace element composition · LA-ICP-MS · IOCG deposit · Kangdian metallogenic province, SW China

Editorial handling: B. Lehmann

Electronic supplementary material The online version of this article (doi:10.1007/s00126-014-0575-7) contains supplementary material, which is available to authorized users.

W. T. Chen (✉) · M.-F. Zhou (✉) · R. Hu
State Key Laboratory of Ore Deposit Geochemistry, Institute of Geochemistry, Chinese Academy of Sciences,
550002 Guiyang, China
e-mail: chenweifly1@163.com
e-mail: mfzhou@hku.hk

W. T. Chen · M.-F. Zhou
Department of Earth Sciences, University of Hong Kong, Pokfulam Road, Hong Kong, China

J.-F. Gao
State Key Laboratory for Mineral Deposits Research, Nanjing University, Nanjing 210093, China

Introduction

The Kangdian Fe-Cu metallogenic province in SW China hosts more than 50 Fe-Cu deposits and extends from Sichuan Province on the north, southward through Yunnan Province

into northern Vietnam (Sun et al. 1991; Zhao and Zhou 2011; Zhou et al. 2014). This province has minimum ore reserves of 600 Mt iron and 5 Mt copper, making it one of the largest Fe-Cu provinces in the world (Qian and Shen 1990; Zhou et al. 2014). In the past decade, the giant Lala, Xikuangshan, Yinachang, and Dahongshan deposits in the region have been regarded as iron-oxide-copper-gold (IOCG) deposits (Li et al. 2002; Zhao and Zhou 2011; Chen and Zhou 2012; Hou et al. 2013), which may have formed from multiple hydrothermal events (~1.7, ~1.45, ~1.05 Ga) (Li et al. 2003a; Zhao and Zhou 2011; Chen and Zhou 2012; Huang et al. 2013a; Ye et al. 2013; Zhao et al. 2013; Zhou et al. 2014). Earlier studies of fluid inclusions and ore compositions suggested that the ore-forming fluids had high salinities and high Na-Ca-K-CO_2 contents (Zhao and Zhou 2011 and references therein; Hou et al. 2013). On the basis of the C-S-O-Pb isotopic compositions of different ore minerals, the fluids were interpreted to have been dominantly magmatic in origin (e.g., Sun et al. 2006; Zhao 2010 and references therein; Zhao and Zhou 2011; Chen and Zhou 2012). However, the nature of the Fe and Cu mineralizing fluids and their genetic relationship, if any, with the coeval intrusions, and the processes by which the magnetite was deposited, were still poorly known.

Previous studies have correlated compositional variations in hydrothermal magnetite with its provenance (e.g., Dupuis and Beaudoin 2011; Nadoll et al. 2014 and references therein; Dare et al. 2014). Recent developments in the application of laser ablation-inductively coupled plasma-mass spectrometry (LA-ICP-MS) now allow in situ analysis of a wide range of trace elements in magnetite with relatively low detection limits (Liu et al. 2008; Nadoll and Koenig 2011; Gao et al. 2013). These investigations demonstrated that trace element compositions of magnetite could provide important information about the origin and characteristics of mineralizing fluids or precursor parental magmas, as well as the processes responsible for magnetite deposition (Frietsch and Perdahl 1995; Müller et al. 2003; Carew 2004; Singoyi et al. 2006; Dupuis and Beaudoin 2011; Dare et al. 2012, 2014; Gao et al. 2013; Nadoll et al. 2014). Magnetite is the dominant ore mineral in the Fe-Cu deposits of the Kangdian metallogenic province (Sun et al. 1991; Zhao and Zhou 2011). In this study, we use the LA-ICP-MS technique to obtain in situ trace element compositions of magnetite from several giant Fe-Cu deposits in the Kangdian metallogenic province. The new dataset allows us to compare compositions of magnetite from different deposits, to constrain possible processes that caused the observed compositional variations, and to understand the genetic relationships between the ore-forming fluids and associated intrusions. We also explore the possible application of trace element compositions of magnetite to provenance studies.

Kangdian IOCG metallogenic province

Regional geology

The Yangtze Block is separated from the Cathaysia Block on the southeast by the Jiangshan-Shaoxing fault (Fig. 1a) and is bounded by the Indochina Block to the southwest, the Tibetan Plateau to the west, and the Qinling-Dabie Orogenic Belt to the north (Fig. 1a). In the Kangdian Province, located in the southwestern part of the Yangtze Block, Proterozoic volcanic-sedimentary sequences crop out along a roughly N-S-trending fault system. These sequences include the Paleoproterozoic Hekou, Dahongshan, and Dongchuan Groups (1.7–1.5 Ga; Greentree and Li 2008; Zhao et al. 2010; Chen et al. 2013; Wang and Zhou 2014) and Meso- to Neoproterozoic Huili, Kunyang, Julin, and Yanbian Groups (~1100–900 Ma; Chen and Chen 1987; Greentree et al. 2006; Geng et al. 2007; Sun et al. 2009; Chen et al. 2014a). These Proterozoic strata are intruded by numerous Proterozoic plutons including ~1.7-Ga gabbroic, ~1.1-Ga gabbroic to granitic, and ~740- to 860-Ma granitic-dioritic-gabbroic intrusions. Both the ~1.7- and ~1.1-Ga intrusions have geochemical affinities of intraplate magmatism and, hence, have been related to rift basins of similar ages (e.g., Greentree et al. 2006; Geng et al. 2007; Zhao 2010; Zhao et al. 2010; Wang et al. 2012; Chen et al. 2014a). On the other hand, the younger Neoproterozoic magmatism has been interpreted to be arc-related (Zhou et al. 2002, 2006) or mantle plume-related (Li et al. 2003b).

Mineralization styles

The Kangdian metallogenic province hosts more than 50 deposits in the Paleoproterozoic Hekou, Dongchuan, and Dahongshan Groups (Sun et al. 1991) (Fig. 1b). Relatively large deposits include Lala, Xikuangshan, Yinachang, E'touchang, and Dahongshan (Sun et al. 1991; Zhao and Zhou 2011). Detailed descriptions of the deposits have been presented elsewhere (e.g., Li et al. 2002; Zhao 2010; Zhao and Zhou 2011 and references therein; Chen and Zhou 2012; Zhao et al. 2013; Zhou et al. 2014). These deposits have comparable mineralization and alteration styles (Sun et al. 1991; Zhao and Zhou 2011). Ore bodies of the deposits are generally lenticular and stratabound and are mostly associated with gabbroic intrusions and hydrothermal breccias (Fig. 1b, c, e) (Zhao 2010; Zhao and Zhou 2011). For example, these deposits have a common paragenetic sequence in which an early Fe-oxide stage of magnetite/hematite mineralization, associated with extensive sodic alteration, is followed by a Cu-sulfide stage of Cu-(Mo, REE, Co, Au, Ag) mineralization, accompanied by potassic and carbonate alteration (Zhou et al. 2014 and references therein).

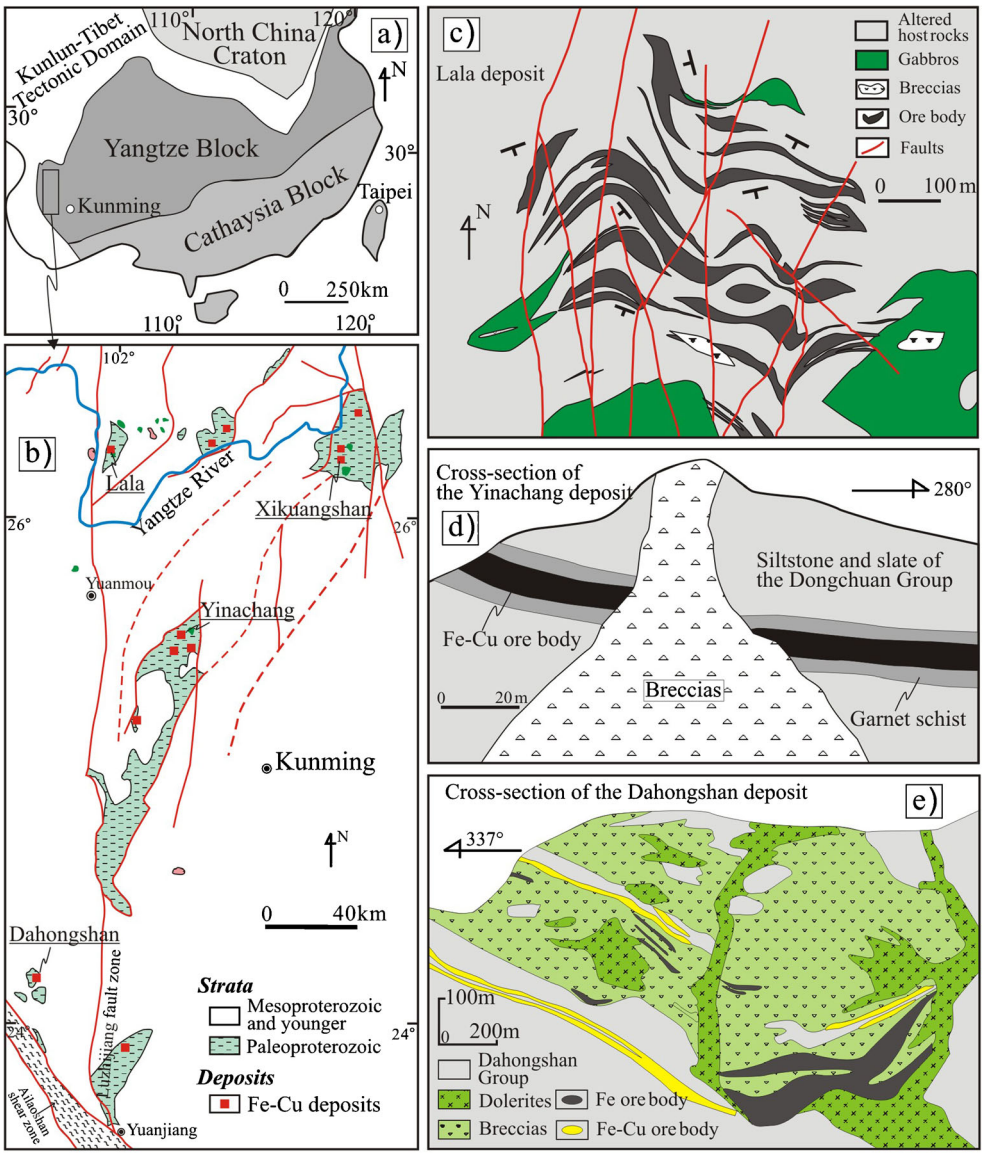

Fig. 1 **a** Tectonic framework of China; **b** Regional geological map of the Kangdian Province showing distribution of Fe-Cu deposits; **c** Simplified geological map of the Luodang open pit of the Lala deposit (at 2036 m level); **d** Cross-section of the Yinachang deposit showing the relationships between Fe-Cu ore bodies and breccias; **e** Cross-section of the Dahongshan deposit showing the relationships among Fe and Fe-Cu ore bodies, dolerite intrusions, and breccias. Panels **b** and **c** are modified after Wu et al. (1990) and Chen and Zhou (2012), respectively, whereas **d** and **e** are modified after Zhao (2010)

Lala deposit

The ~1.1-Ga Lala Fe-Cu deposit contains more than 200 million tons of ores with an average grade of 13 wt% Fe, 0.92 wt% Cu, 0.018 wt% Mo, 0.022 wt% Co, 0.25 wt% REE_2O_3, and 0.16 ppm Au (Zhu et al. 2009). The ore bodies occur as irregular lenses and veins in albitites, schists, carbonates, and quartzites of the Hekou Group and are spatially associated with ~1.7- and ~1.1-Ga gabbroic intrusions (Zhu 2011; Chen et al. 2013) (Fig. 1c). The ore bodies are mostly stratabound, and minor are controlled by faults or shear zones. Breccias are locally present in the Lala deposit where they are generally associated with ore bodies. They are composed of irregular blocks of hosting strata that are cemented by hydrothermal minerals, including albite, magnetite, sulfides, and calcite. The ores can be classified as magnetite, sulfide, and mixed magnetite-sulfide ores on the basis of different concentrations of ore minerals (Fig. 2a, b). These ores are generally massive, disseminated, and banded, but they may also occur as stringers or stockworks crosscutting the hosting rocks (Fig. 2a, b). The deposit has a paragenetic sequence of early Fe-oxide stage forming magnetite, apatite, and albite and late Cu-sulfide stage forming chalcopyrite, pyrite, bornite, molybdenite, REE minerals (e.g., monazite, bastnaesite, and xenotime) (Cu-sulfide stage). The Fe-oxide stage is associated with Na-Fe alteration, whereas the Cu-sulfide stage is accompanied by K-Ca-carbonate alteration (Chen and Zhou 2012). Magnetite grains of the Fe-oxide stage are subhedral to anhedral and closely associated with variable amounts of apatite and albite (Fig. 3a). Some anhedral magnetite grains are also intergrown with, or enclosed in, chalcopyrite in the Cu-sulfide stage (Fig. 3b). Hematite in the Lala deposit occurs as

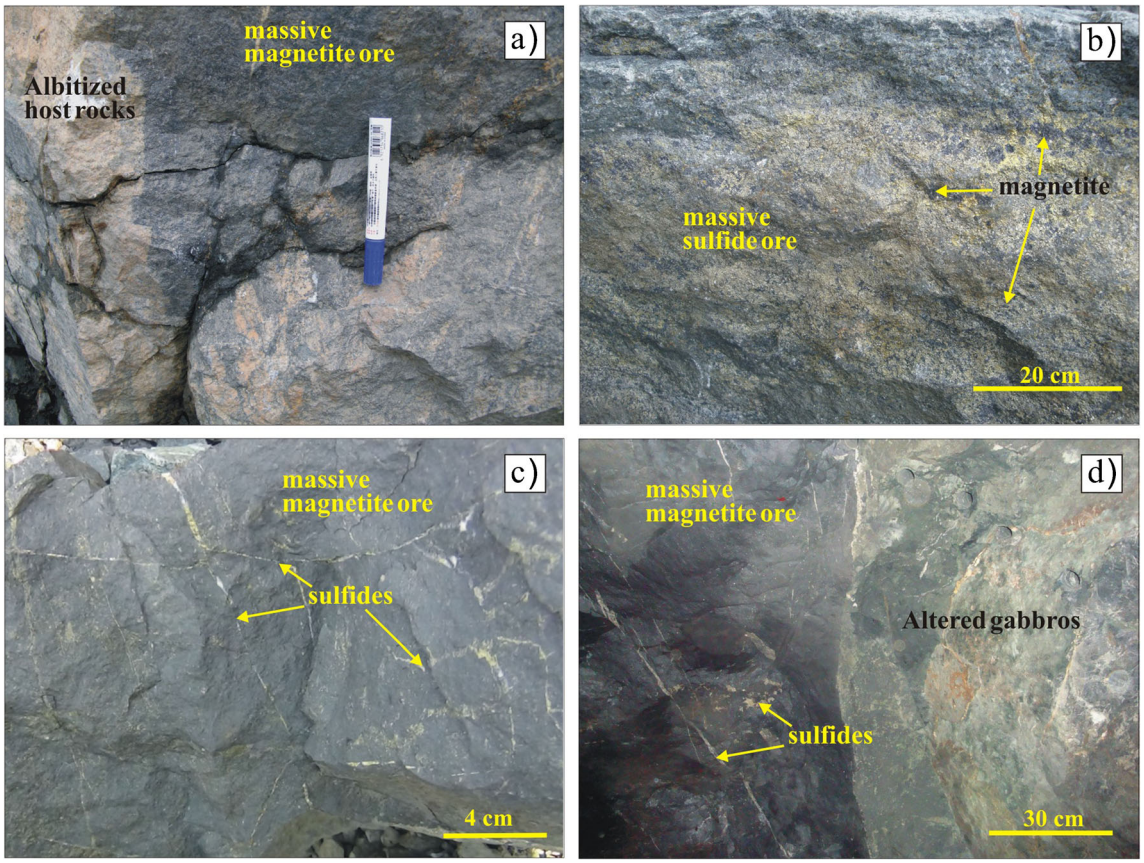

Fig. 2 Field photos of various ores from different deposits in the Kangdian Province. **a**, **b** Massive oxide and sulfide ores in the Lala deposit. Note that the oxide ores are in sharp contact with host rocks, and minor magnetite grains are also present in massive sulfide ores; **c** Massive magnetite ores in the Yinachang deposit. There are also minor sulfide veinlets crosscutting the magnetite ores; **d** Massive magnetite ores in contact with altered gabbroic rocks in the Dahongshan deposit. There are also disseminated sulfides in the magnetite ores

veins or patches crosscutting or overprinting the Fe-(Cu) ores and is paragenetically younger than the Fe and Cu mineralization.

Yinachang deposit

The ~1.65-Ga Yinachang deposit contains approximately 15 Mt of Cu ores with 0.85–0.97 wt% Cu and 20 Mt of Fe ores with 41.9–44.5 wt% Fe, accompanied by trace amounts of Co, Mo, and REE (local exploration report). Ore bodies are hosted in the Paleoproterozoic Dongchuan Group, occurring either along fault planes or lithologic contacts in NE- or NNE-trending anticlines (Sun et al. 1991). The ore bodies are spatially associated with synchronous doleritic intrusions (Guo et al. 2014) and with hydrothermal breccias, which either intrude the ore bodies or are crosscut by them (Fig. 1d) (Hou et al. 2013; Ye et al. 2013; Zhao et al. 2013).

There are mainly fine-grained massive or banded magnetite-chalcopyrite ores with subordinate banded hematite ores in the Yinachang deposit (Zhao et al. 2013). The field relationships between the magnetite and hematite ores are not clear, even though some magnetite grains are locally replaced by hematite. In magnetite-chalcopyrite ores, it is clear that early magnetite patches have been crosscut by sulfide veins (Fig. 2c). The mineralization sequence consists of an early Fe-oxide stage of Fe-(REE) mineralization dominated by magnetite, albite, and siderite with subordinate REE-rich apatite, fluorite, and ankerite (e.g., Fig. 3c), followed by a Cu-sulfide stage of Cu-(Mo, REE) mineralization with abundant chalcopyrite, pyrite, molybdenite, and subordinate REE-bearing minerals (e.g., monazite, bastnaesite, and parisite) and trace amounts of Nb- and U-bearing minerals (Hou et al. 2013; Zhao et al. 2013). Pervasive albitization preceded magnetite precipitation and continued during the Fe-oxide stage, similar to that of the Lala deposit. Magnetite in the Fe-oxide stage is subhedral to anhedral with variable sizes (Fig. 3c) and appears to slightly predate apatite and/or fluorite. We did not identify any magnetite grains in the Cu-sulfide stage.

Dahongshan deposit

Early exploration indicates that the ~1.65-Ga Dahongshan deposit has a reserve of 458 Mt of ores with 41 wt% Fe and 1.35 Mt Cu (metal) with Au, Ag, Co, Pd, and Pt as potential

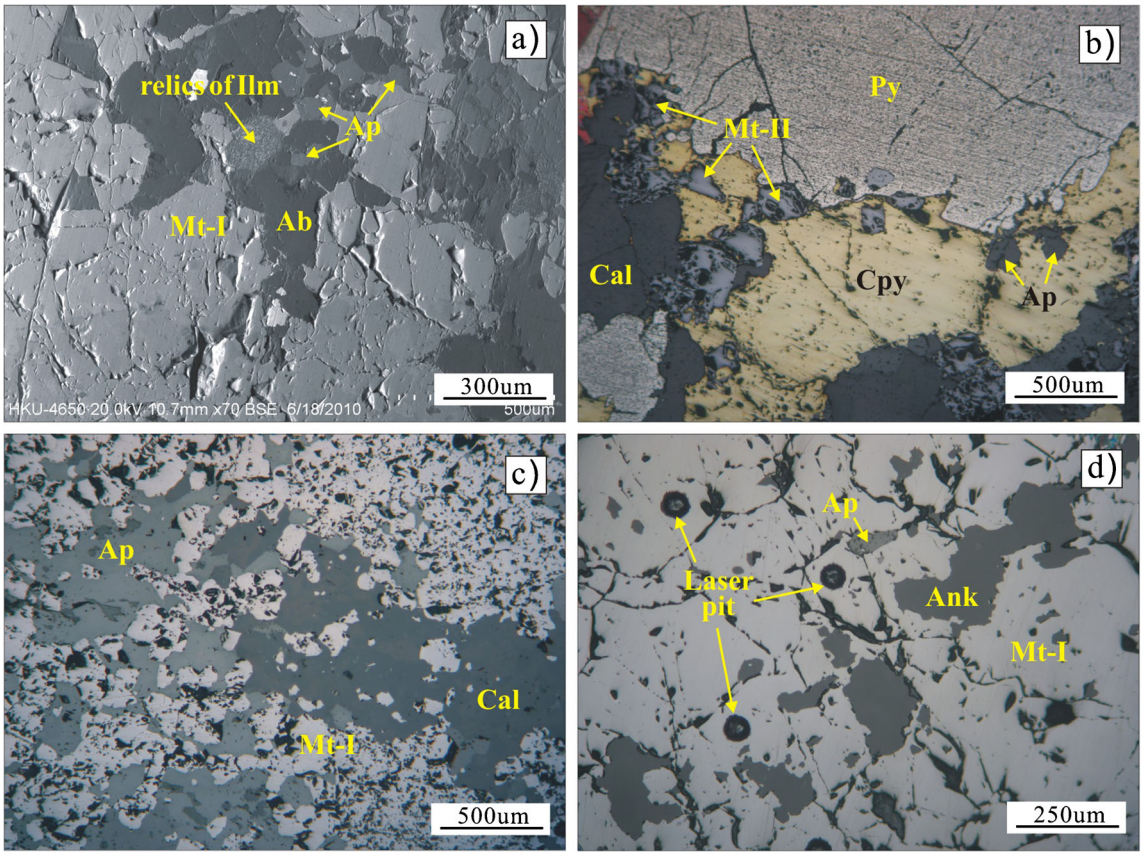

Fig. 3 Photomicrographs of different ores from different deposits. **a** Oxide ore in the Lala deposit composed dominantly of magnetite, albite, and apatite. Note that there are minor relics of partly replaced ilmenite. BSE image: **b** Sulfide ore in the Lala deposit consisting of pyrite, chalcopyrite, and calcite with minor magnetite and apatite. Note that some magnetite grains are euhedral, slightly predating the sulfides. Reflected light: **c** Oxide ore in the Yinachang deposit composed of intergrown grains of magnetite, apatite, and albite. Reflected light: **d** Massive magnetite ore in the Dahongshan deposit consisting of magnetite, apatite, and ankerite. Also shown are laser pits. Mineral abbreviations: *Mt* magnetite, *Cal* calcite, *Cpy* chalcopyrite, *Py* pyrite, *Ap* apatite, *Ank* ankerite, *Ab* albite, *Ilm* ilmenite

by-products (unpublished exploration report of Yunnan Province 1983). Some Fe-(Cu) ore bodies are roughly concordant with the stratification of the Paleoproterozoic Dahongshan Group but are spatially associated with coeval gabbroic/doleritic plutons intruding the strata (Fig. 2d) (Zhao and Zhou 2011). Although it is controversial, Zhao (2010) show that most of Fe ore bodies are apparently hosted in a doleritic breccia pipe related to intrusion of coeval mafic magmas (Figs. 1e and 2d).

Both host rocks and Fe-(Cu) ores are generally foliated, and some of them have been metamorphosed to the lower amphibolite facies. The Fe-oxide ores have massive or banded textures and are crosscut by veinlets of sulfides (Fig. 2d). There are also stratabound disseminated magnetite-sulfide ores in which magnetite predates the Cu-sulfides (Zhao 2010). This deposit has a paragenetic sequence similar to that of the Lala deposit, including an early Fe-oxide stage of magnetite, apatite, albite, and ankerite (Fig. 3d) and a late Cu-sulfide stage of chalcopyrite and minor bornite closely associated with calcite, biotite, and sericite (Cu-sulfide stage). The Fe-oxide stage is accompanied by extensive albitization, followed by alteration of amphibole, tourmaline, biotite, sericite, carbonate, and chlorite in the Cu-sulfide stage.

Sampling and analytical methods

Magnetite from the Lala, Yinachang, and Dahongshan deposits was selected for trace element analyses. Most of the analyzed magnetite grains are intergrown with albite and/or apatite and thus should be the products of the early Fe-oxide stage (Fig. 3a, c, d). Minor magnetite grains of the Cu-sulfide stage in the Lala deposit were also analyzed for comparison with those from the Fe-oxide stages of these deposits.

Trace elements of magnetite were determined with a Coherent GeoLasPro 193-nm Laser Ablation system coupled with an Agilent 7700x ICP-MS at the State Key Lab of Ore Deposit Geochemistry, Institute of Geochemistry, Chinese Academy of Sciences, Guiyang, China. Detailed operating conditions for the laser ablation system and the ICP-MS instrument, as well as data reduction, have been described by Gao et al. (2013) and Huang et al. (2013b). Helium was

applied as a carrier gas and argon as a makeup gas mixed with the carrier gas via a T-connector before entering the ICP. Each analysis utilized laser spots 60 μm in diameter with successive pulses at 4 Hz. Each analysis included a background acquisition of approximately 20 s for a gas blank, followed by data acquisition of 40 s from the sample. Element contents were calibrated against multiple reference materials (GSE-1G, BCR-2G, BIR-1G, BHVO-2G, and NIST610) using ^{57}Fe as the internal standard (Gao et al. 2013). Every eight analyses were followed by one analysis of GSE-1G to correct time-dependent drift of sensitivity and mass discrimination. The sum of all element concentrations expressed as oxides (according to their oxidation states in magnetite) are considered to be 100 wt% for a given anhydrous mineral (Liu et al. 2008).

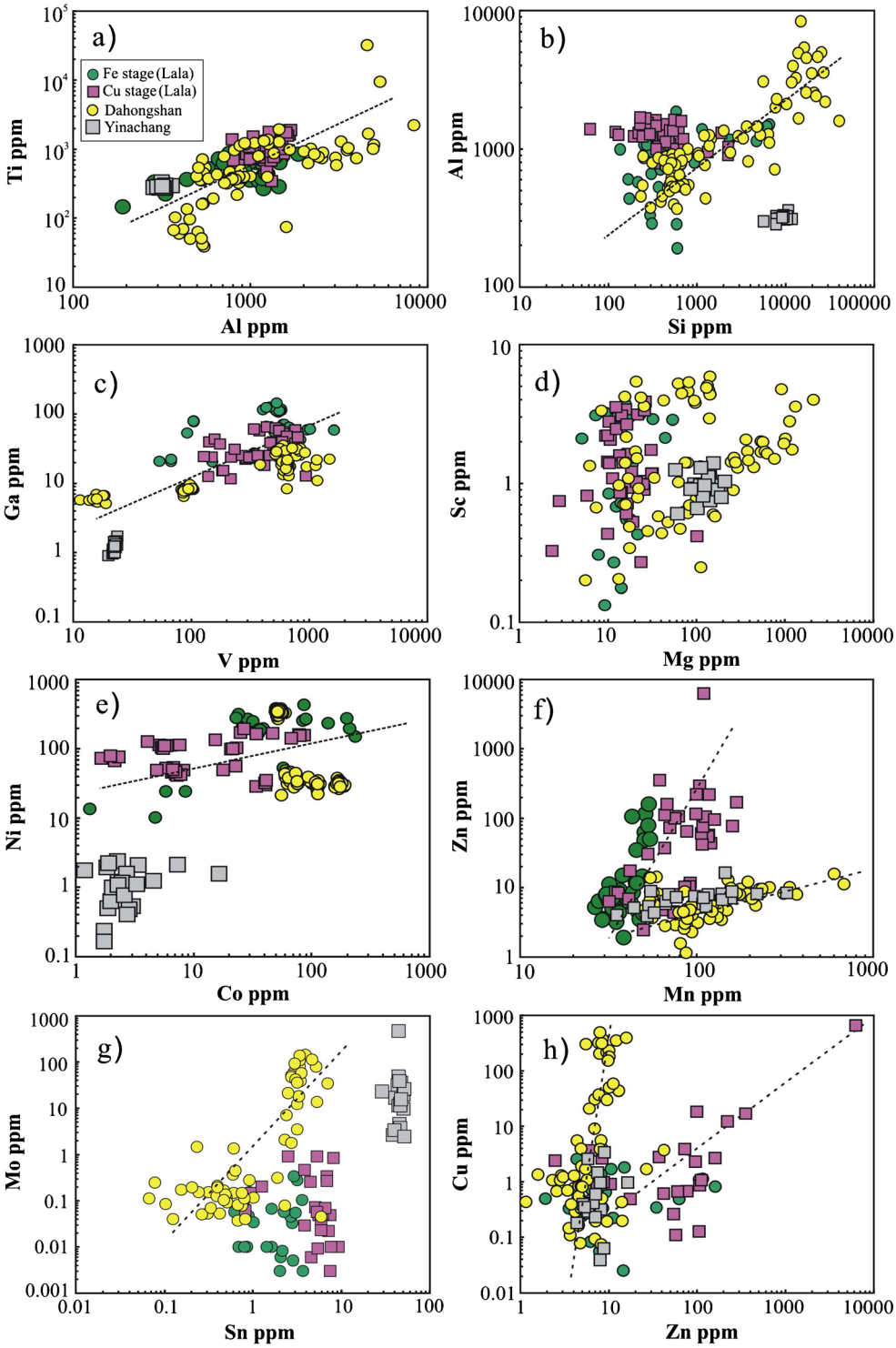

Fig. 4 Bimodal plots of Ti vs. Al (**a**), Al vs. Si (**b**), Ga vs. V (**c**), Sc vs. Mg (**d**), Ni vs. Co (**e**), Zn vs. Mn (**f**), Mo vs. Sn (**e**), and Cu vs. Zn (**f**) in magnetite from different deposits

Offline data reduction was performed with ICPMSDataCal (Liu et al. 2008), including integration selection of background and analysis signals, time drift correction, and quantitative calibration. The ratio $Fe^{2+}/\Sigma Fe$ of 0.33 was used for data reduction based on magnetite compositions obtained by Chen and Zhou (2012). All the analyses of magnetite samples and standards are provided in Appendix I, which is available online.

Analytical results

Lala deposit

Magnetite formed during the Fe-oxide and Cu-sulfide stages from the Lala deposit contains substantial Mg, Al, Si, Ca, Ti, Mn, V, Co, Ni, Sn, and Ga (Appendix I; Fig. 4). Concentrations of other elements, such as Sc, Cr, Zn, Ge, Mo, Zr, W, Cu, and Pb, are either close to, or below, detection limits, or exhibit considerable intergrain variation (Appendix I). Magnetite grains from both stages have comparable ranges of Al (~200–2000 ppm), Ti (~100–2000 ppm), Mo (~0.01–1 ppm), and V (~40–2000 ppm) (Appendix I; Fig. 4). In general, Ga exhibits a stronger affinity for magnetite in the Fe-oxide stage, whereas Sn, Cu, and Mn are typically higher in magnetite of the Cu-sulfide stage (Appendix I; Fig. 4). However, the V, Ti, Si, Sc, Mg, Zn, Al, and Mo do not show significant distinctions between magnetite from the two stages (Appendix I; Fig. 4). There are positive correlations between trace element pairs for magnetite from both stages, such as Ti vs. Al, Ga vs. V, Zn vs. Mn, and Cu vs. Zn (Fig. 4a, c, f, h).

For a comparison purpose, trace element concentrations of magnetite are normalized against that from the El Laco deposit, Chile (Nystrom and Henriquez 1994). Magnetite grains from the Fe-oxide and Cu-sulfide stages have indistinguishable patterns (Fig. 5a), similar to those of magnetite in the Lightning Creek IOCG deposit, Cloncurry, Australia, but different from those of Kiruna-type deposits in Chile and Sweden (Frietsch and Perdahl 1995).

Yinachang deposit

Magnetite grains in the Fe-oxide stage of the Yinachang deposit have compositions different from those in the same stage of the Lala deposit (Figs. 4 and 5). They have much lower Co (<3 ppm) and Ni (mostly <6 ppm) (Fig. 4e), but contain much higher Mo (>2 ppm) and Sn (>30 ppm) (Fig. 4g). There are positive correlations between Zn and Mn and between Cu and Zn in both deposits (Fig. 4f, h). The compositional differences of magnetite in the Fe-oxide stage from the two deposits are also reflected in the multielement diagram (Fig. 5c) where the magnetite from the Yinachang deposit exhibits pronounced depletions of V and Ni (Fig. 5c).

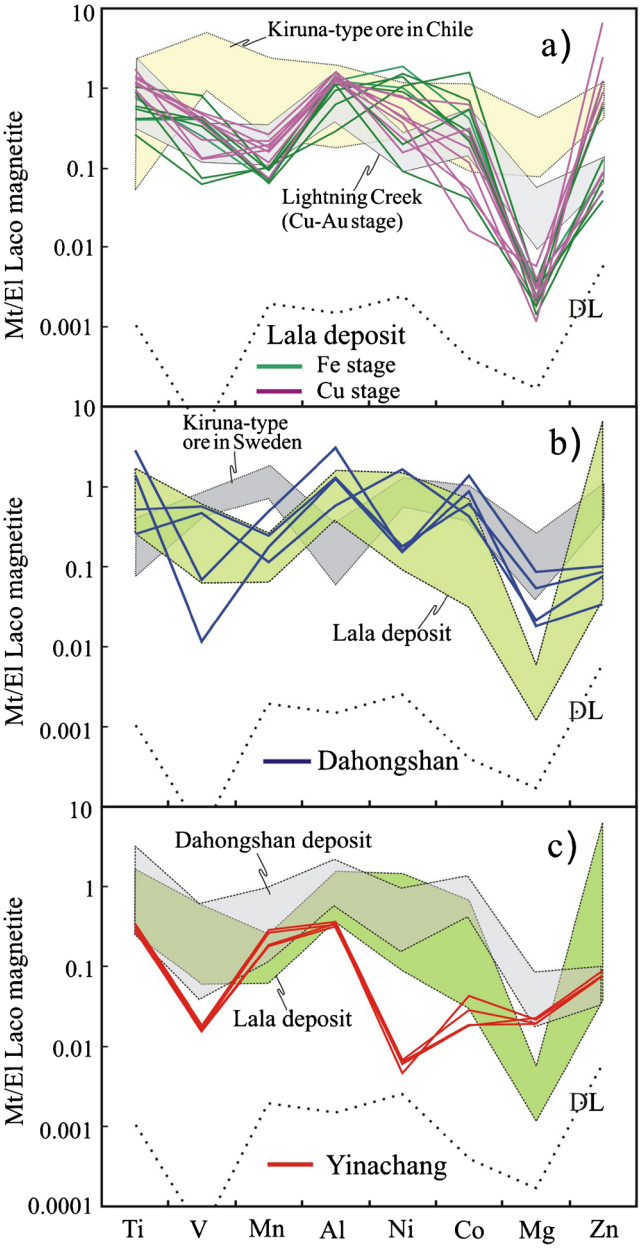

Fig. 5 Normalized multielemental patterns of magnetite from the Lala (both the Fe-oxide and Cu-sulfide stages) (**a**), Yinachang (**b**) and Dahongshan (**c**) deposits. Also plotted are magnetite from Kiruna-type ores in Chile and Sweden (Frietsch and Perdahl 1995) and Cu-Au ores in Lightning Creek, Australia (Carew 2004). Normalizing values are the average composition of magnetite from the El Laco Kiruna-type deposit, Chile (Nystrom and Henriquez 1994): Ti=933, V=1360, Mn=486, Al=944, Ni=201, Co=124, Mg=5990, and Zn=90 (all in ppm). Fe stage: Fe-oxide stage; Cu stage: Cu-sulfide stage

Dahongshan deposit

Magnetite grains in the Fe-oxide stage from the Dahongshan deposit have concentrations of most trace elements quite similar to those in the same stage of the Lala deposit (Figs. 4 and 8). For example, they show similarly large variations in Al (~300–10,000 ppm), Ti (~30–100,000 ppm), Si (~200–40,

000 ppm), V (~10–2000 ppm), Mg (~5–4000 ppm), and Mn (~50–10,000 ppm) (Fig. 4). However, in general, the Dahongshan magnetites have Ga (~5–30 ppm) and Zn (~1–20 ppm) contents slightly lower, but Sc (~0.1–10 ppm), Mo (~0.03–200 ppm), and Co (~50–200 ppm) contents higher than those in the same stage of the Lala deposit (Fig. 4). Positive correlations between trace element pairs, such as Ti vs. Al, Al vs. Si, Ga vs. V, Mo vs. Sn, Cu vs. Zn, and Zn vs. Mn are common (Fig. 4a–c, f–h). In the multi-element diagram, Dahongshan magnetites have patterns that are roughly similar to those of the Lala deposit, except for Co and Zn, which are higher and lower, respectively (Fig. 5).

Discussion

Possible controls on composition of hydrothermal magnetite

In addition to fluid composition, which is the major controls on the composition of hydrothermal magnetite, other potential influences may include (1) host rock composition due to fluid-rock interaction, (2) nature of coprecipitating minerals, and/or (3) intensive parameters (e.g., temperature and oxygen fugacity (fO_2)) during mineral formation (Nystrom and Henriquez 1994; Frietsch and Perdahl 1995; Toplis and Corgne 2002; Carew 2004; Dupuis and Beaudoin 2011; Dare et al. 2014; Nadoll et al. 2014). Therefore, in order to constrain the nature and origin of the ore-forming fluids using magnetite compositions, the first step is to understand whether, and to what extent, these controls affect trace element compositions of magnetite from these deposits.

Fluid-rock interaction

Magnetite formed during fluid-rock interaction or replacement may "inherit" some elemental characteristics of the hosting rocks (c.f. Carew 2004; Nadoll et al. 2014). The ores forming at the Fe-oxide stages of the Lala and Dahongshan deposits are hosted dominantly in albitites, siltstones, and carbonates, whereas those of the Yinachang deposit are mainly hosted in siltstones and slates (Zhao and Zhou 2011; Hou et al. 2014; Zhou et al. 2014). In order to investigate the effect of host rock compositions on magnetite chemistry, all the magnetite samples are plotted according to lithology of host rocks (Fig. 6).

In the plots, magnetite grains of ores hosted in albitites have higher Sc and Ga but lower Mn than those hosted in siltstones, whereas magnetite grains of ores hosted in carbonates have concentrations of Mg and Mn similar to those of ores hosted in albitites but much lower than those of ores hosted in siltstones (Fig. 6e, f). These plots suggest that the observed compositional variations cannot be explained solely by differences of host rocks lithology. The reason is that if that was the case, magnetites hosted in carbonates (having relatively high Mg and Mn) should contain much higher Mg and Mn than those hosted in albitites and siltstones (Fig. 6e, f). In contrast, the good correlations of Mg and Mn with Sc and Zn are best ascribed to differentiation of the ore-forming fluids (Fig. 6e, f).

Concentrations of V, Ti, Al, and Cr in magnetite of ores hosted in different host rocks are relative, and there are roughly positive correlations between V and Ga (Fig. 4c) and Ti and Al (Fig. 4a). These correlations indicate that fluid-rock interaction played a very limited role in abundances of these elements. However, the scattered Ti and Cr in the Ti vs. V and Cr vs. V plots (Fig. 6a) may partly reflect chemical influences from the host rocks. Indeed, magnetite grains of ores hosted in siltstones do have higher Ti concentrations than those of ores hosted in carbonates and albitites, lithologies with relatively low TiO_2 contents (Fig. 6a, d). In the siltstones, there is abundant textural evidence that the original ilmenite or titanomagnetite grains have been replaced by magnetite and other hydrothermal minerals (e.g., Fig. 3a). Due to extremely low solubility of Ti and Cr in the fluids, it is reasonable to consider that these high Ti-Cr minerals may have contributed Ti to the newly precipitated magnetite grains, particularly those Ti-Cr-rich magnetite rains, during fluid-rock interaction.

In summary, variable concentrations of such elements as Cr, V, Co, Mg, Mn, Sc, Ga, and Al in magnetite are limitedly controlled by host rock compositions during fluid-host rock interaction. Only Ti concentrations appear to reflect, at least in part, fluid-host rock interaction. We consider that the limited influences from host rock chemistry are possibly due to the fact that most magnetite ores in these deposits was not formed by replacing host rocks (e.g., Fig. 2c, d) (Chen and Zhou 2012).

Precipitation of coexisting minerals

Minerals coprecipitated with magnetite may affect concentrations of some trace elements within the magnetite due to different partition coefficients (Dare et al. 2014; Nadoll et al. 2014). For example, chalcophile elements may be partitioned preferentially into sulfides compared to magnetite (Dare et al. 2014). However, such an effect related to element partitioning would have been very limited for magnetite in the Fe-oxide stage of these deposits because the stage has a simple mineral assemblage dominated by magnetite, albite, and apatite. Indeed, Ti, V, Cr, Co, Ni, Mo, Cu, and Zn are highly compatible in magnetite relative to apatite or albite, and thus, their concentrations would have been a little affected by coprecipitating albite or apatite (Neilson 2003). In the Cu-sulfide stage of the Lala deposit,

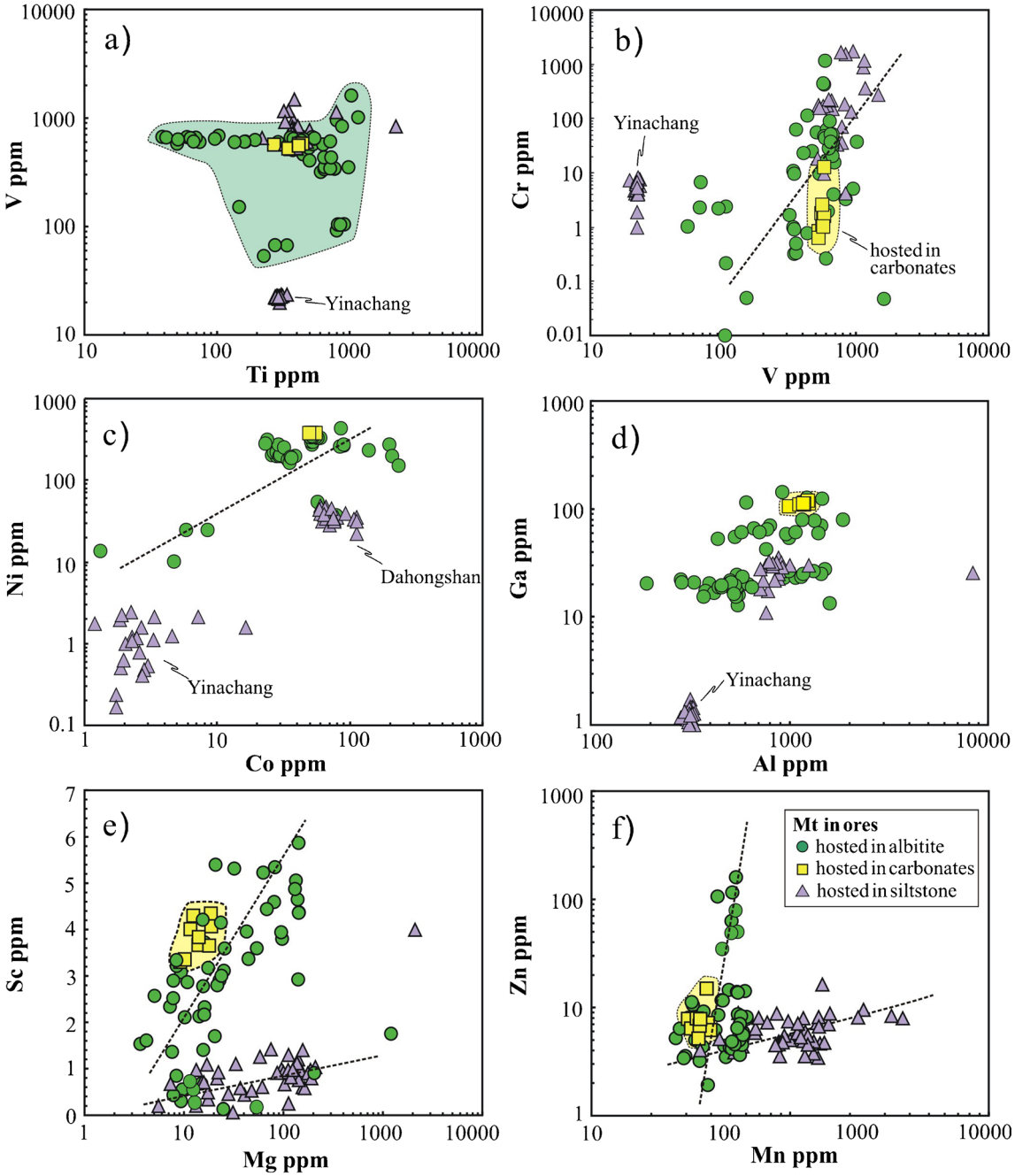

Fig. 6 Bimodal plots of V vs. Ti (**a**), Cr vs. V (**b**), Ni vs. Co (**c**), Ga vs. Al (**d**), Sc vs. Mg (**e**), and Zn vs. Mn (**f**) of magnetite hosted in different lithologies from different deposits. Plotted analyses include those of magnetite hosted in siltstone (from the Dahongshan and Yinachang deposits), albitite, and carbonates (from the Lala deposit). Fe stage: Fe-oxide stage; Cu stage: Cu-sulfide stage

however, it is expected that coprecipitation of sulfides would have greatly decreased the abundance of these elements for incorporation in magnetite. Interestingly, magnetite of the Cu-sulfide stage has Co, Ni, and Mo contents similar to those of the Fe-oxide stage, and Zn and Cu contents are even significantly higher (Fig. 4e–h). This feature may be explained by two possibilities: (1) precipitation of sulfides in these ores did not significantly affect concentrations of Zn and Cu in magnetite, or (2) the fluids of the Cu-sulfide stage have extremely high concentrations of these elements. The first possibility is favored on the basis of the facts that magnetite from both stages have almost overlapped normalized elemental patterns (Fig. 5a) and magnetite in the Cu-sulfide stage did crystallize slightly earlier than the sulfides (Fig. 3b). In summary, the trace element concentrations of magnetite grains from both the Fe-oxide and Cu-sulfide stages of the Fe-Cu deposits were not significantly affected by coprecipitating minerals.

Intensive parameters, T and fO_2

The effects of various intensive parameters (e.g., *T* and fO_2) on the concentrations of trace elements in hydrothermal magnetite are currently poorly constrained (e.g., Ilton and Eugster 1989; Toplis and Corgne 2002; Nadoll et al. 2014). Ilton and Eugster (1989) showed experimentally in a system composed of magnetite and supercritical chloride-rich fluids at 600–800 °C and 2 kb that Cu, Zn, and Mn are preferentially enriched into the evolved fluids at lower temperatures. This is consistent with our finding that in the Lala deposit, magnetite grains of the Cu-sulfide stage (300–400 °C) have Cu, Zn, and Mn contents higher than those of the Fe-oxide stage (385–450 °C) (Fig. 4f, h) (Chen and Zhou 2012). However, this does not necessarily mean that the temperature influences the partition coefficients of these elements in magnetite but just indicates that these elements are incompatible in magnetite during fluid evolution.

fO_2 may impact the partitioning of elements with several valence states, such as V and Sn. For example, increasing fO_2 could decrease the partition coefficient of V (with +3, +4, and +5 valences) into magnetite in an iron-rich melt/liquid (Toplis and Corgne 2002). In contrast, Sn (in the quadrivalent state) may substitute more readily for Fe^{3+} in magnetite under more oxidized condition (Goldschmidt 1958; Carew 2004). Shentu (1997) and Jin and Shen (1998) reported, on the basis of fluid inclusion and mineral composition studies, that fluids of the Cu-sulfide stage in the Lala deposit were more oxidized than those of the Fe-oxide stage. However, comparable V and Sn contents in magnetite from both the Fe-oxide and Cu-sulfide stages of the Lala deposit (Fig. 7a) suggest a little impact from changing fO_2 conditions. This interpretation is further supported by the poor negative correlation between V and Sn of magnetite from the Lala and Dahongshan deposits (Fig. 7a). Therefore, the variable abundances of V and Sn in magnetite of both stages are more likely controlled by variable contents of these elements in the fluids.

In summary, although T and fO_2 do affect some elements such as Cu, Mn, Zn, V, and Sn, our results well indicate that variations of these elements in magnetite were mainly controlled by fluid compositions. In combination with our earlier interpretations on the potential effects of fluid-rock interaction and coprecipitating minerals, we propose that fluid composition is the principal control on the variations of many trace elements in magnetite grains from different deposits of the Kangdian Province. As such, concentrations of these elements can be used to explore the nature and origin of the ore-forming fluids for the Fe-oxide stage of these deposits and Cu-sulfide stage of the Lala deposit, as will be discussed below.

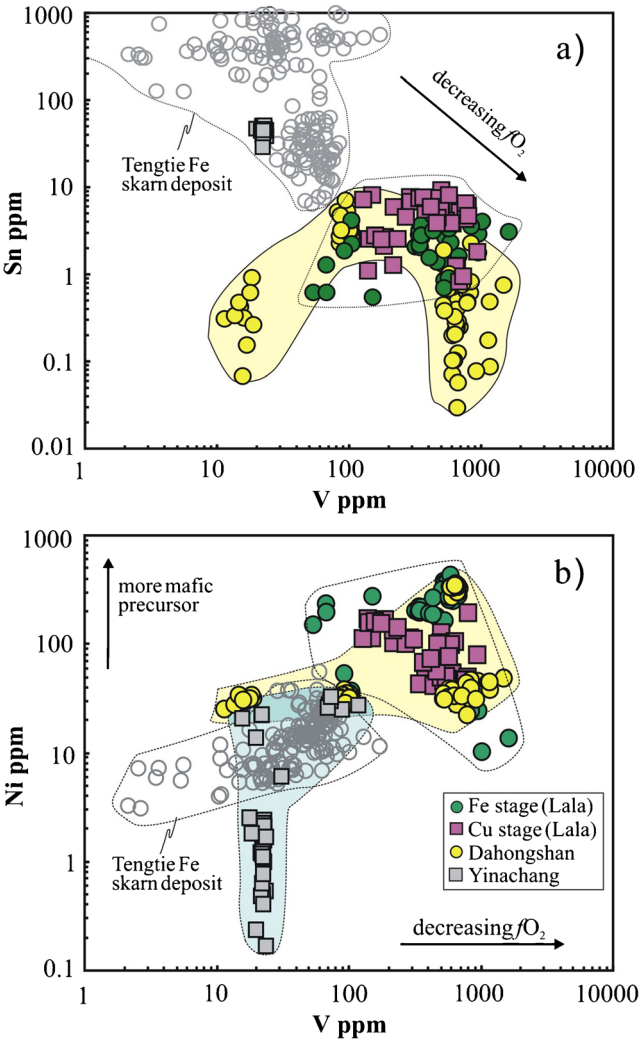

Fig. 7 Plots of **a** Sn vs. V and **b** Ni vs. V showing compositions of magnetite from different deposits. Also plotted are the compositions of magnetite grains from the Tengtie granite-related Fe skarn deposit, SE China (Zhao and Zhou 2015). It is noted that magnetite from the Yinachang deposit has the lowest Ni and V but highest Sn, roughly overlapping with those of the Fe skarn deposit. Fe stage: Fe-oxide stage; Cu stage: Cu-sulfide stage

Implications for the nature and origin of ore-forming fluids

Many C-O-S-Pb isotopic studies of the Fe-Cu deposits in the Kangdian Province indicate that the ore-forming fluids of these deposits were dominantly magmatic in origin (e.g., Sun et al. 2006; Zhao and Zhou 2011 and references therein; Chen and Zhou 2012). However, it is not known whether the ore-forming fluids of the different stages were evolved from a similar magmatic source or whether multiple sources were involved (Zhao and Zhou 2011). Trace element data of magnetite reported in this study provide constrains on these poorly known issues.

Ore-forming fluids of the Fe-oxide stage of different deposits

Magnetite grains in the Fe-oxide stages of both the Dahongshan and Lala deposits have similar concentrations of many trace elements (Fig. 4) and normalized trace element patterns (Fig. 5b), particularly in terms of Ti, Al, Mg, V, Cr, Ga, Sc, Co, Ni, Zn, Cu, and Sn. In combination with the similar mineralization styles and host rocks for the Fe-oxide stages in both deposits (Zhao and Zhou 2011; Chen and Zhou 2012; Chen et al. 2014b), we suggest that their magnetite grains could have formed from chemically similar ore-forming fluids, even though magnetite grains in the Fe-oxide stage of the Dahongshan deposit have slightly higher Mo contents, possibly due to the slightly evolved feature of the fluids (c.f. Nadoll et al. 2014). In addition, magnetite grains in the two deposits have also similarly high Ni contents compared to some granite-related Fe skarn deposits (Zhao and Zhou 2015) (Fig. 7b), supporting the previous view that the ore-forming fluids were genetically related to mafic magmas that formed coeval intrusions in the region (e.g., He 1980; Zhao 2010; Zhao and Zhou 2011). This is because Ni-rich fluids are suggested to be commonly evolved from relatively mafic magmas (Goldschmidt 1958; Carew 2004).

Magnetite grains in the Fe-oxide stage of the Yinachang deposit have concentrations of V, Ni, Co, Mo, and Sn and normalized trace elemental patterns quite different from those of the same stage in the Lala and Dahongshan deposits (Figs. 4 and 5c), indicating their formation from a chemically different fluid possibly derived from different magma sources. For example, they have much lower V but higher Sn and Mo contents relative to those of the Lala and Dahongshan deposits (Fig. 7), suggesting that they have precipitated from a relatively oxidized, Mo-rich fluid (White et al. 1981; Toplis and Corgne 2002), as shown earlier. Local presence of molybdenite in the Fe-oxide stage of the Yinachang deposit (Zhao et al. 2013) further supports that the fluid is relatively Mo-rich compared to those of the Lala and Dahongshan deposits. Notably, magnetite of the Yinachang deposit has much lower Ni contents than those of the Lala and Dahongshan deposits but similar to magnetite in the granite-related Fe skarn deposit (Zhao and Zhou 2015) (Fig. 7b). These features provide evidence for the ore-forming fluid of the Yinachang deposit to have been evolved from relatively felsic magmatic sources compared to those of the Lala and Dahongshan deposits (e.g., Carew 2004). Therefore, our results may argue against a previous view that the fluids of the Yinachang deposit are genetically related to the spatially associated mafic intrusions in the region (e.g., Hou et al. 2013, 2014).

Ore-forming fluids of the Cu-sulfide stage of the Lala deposit

On the basis of Sr isotopic compositions, our early study speculated that the fluid of the Cu-sulfide stage may have evolved from a magma source different from that of the fluid of the Fe-oxide stage of the Lala deposit (Chen et al. 2014b). However, except Cu, Zn, and Mn, magnetite grains of the Cu-sulfide stage do not exhibit large differences of trace elemental compositions or normalized patterns when compared to those of the Fe-oxide stage (Figs. 4 and 5a). This similarity seems to indicate that the ore-forming fluids for both the Fe-oxide and Cu-sulfide stages should have been derived from a common source, thus arguing against our early speculation. Indeed, slightly higher Cu, Zn, and Mn contents of magnetite in the Cu-sulfide stage (Fig. 6) can be easily explained by their precipitation from relatively low-temperature, Cu, Zn, and Mn-enriched fluids evolved from the fluids of the early Fe-oxide stage (c.f. Dare et al. 2014). Nevertheless, because these magnetite grains of the Cu-sulfide stage predate slightly the sulfides of this stage (Fig. 2b), our result cannot rule out the possibility that the evolved Fe mineralizing fluid has mixed with external Cu-Mo-rich fluids after magnetite precipitation.

Using magnetite compositions for provenance discrimination

Previous studies of trace elements in magnetite have shown that they can be used to identify ore-forming environments, ore deposit types, and genesis of mineral deposits (Pearce and Gale 1977; Dupuis and Beaudoin 2011; Carranza et al. 2012; Dare et al. 2014; Nadoll et al. 2014). Many elements in magnetite, including Ni, Cr, Si, Mg, Ca, Ti, V, and Mn, have been used to distinguish magmatic and hydrothermal mineral deposit types, including IOCG, Kiruna apatite-magnetite, banded iron formation (BIF), porphyry Cu, Fe-Cu skarn, magmatic Fe-Ti-V-Cr or Ni-Cu-PGE, Cu-Zn-Pb volcanogenic massive

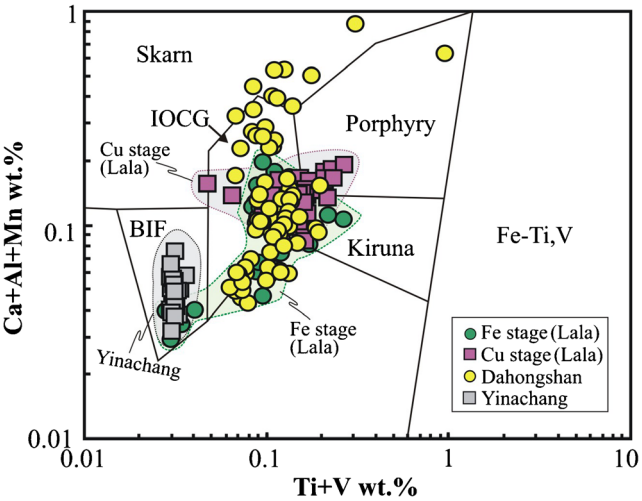

Fig. 8 Plots of V+Ti vs. Ca+Al+Mn of magnetite from the Lala, Yinachang and Dahongshan deposits. Reference fields are after Dupuis and Beaudoin (2011). *BIF* banded iron formation; *Skarn* Fe-Cu skarn deposits; *IOCG* iron-oxide-copper-gold deposits; *Porphyry* porphyry Cu deposits; *Kiruna* Kiruna apatite-magnetite deposits; *Fe-Ti, V* magmatic Fe-Ti-oxide deposits. Fe stage: Fe-oxide stage; Cu stage: Cu-sulfide stage

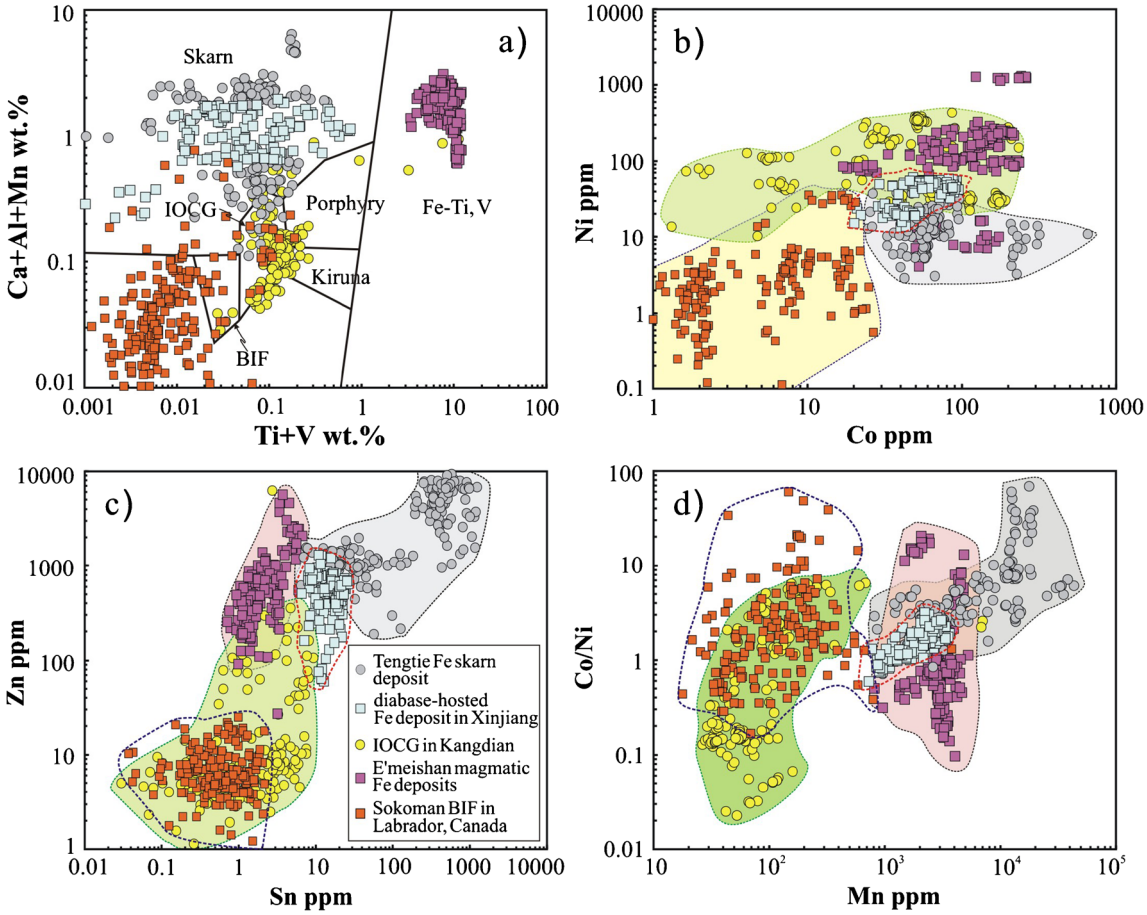

Fig. 9 Plots of Ca+Al+Mn vs. Ti+V (**a**), Ni vs. Co (**b**), Zn vs. Sn (**c**), and Co/Ni vs. Mn (**d**) in magnetite from different types of deposits including IOCG deposits in Kangdian; Fe skarn deposits in Tengtie, SE China (Zhao and Zhou 2015); diabase-hosted Fe deposit in Xinjiang, NW China (Huang et al. 2013b); Sokoman iron formation in Labrador, Canada (Chung et al. 2015); and magmatic Fe-Ti oxide deposits in Emeishan, SW China (Liu et al. 2015). Note that plots of Dupuis and Beaudoin (2011) (**a**) can be used to discriminate magmatic oxide deposits from other hydrothermal deposits. The Co-Ni, Zn-Sn, and Co/Ni-Mn plots can sufficiently discriminate Fe-Cu deposits from Fe skarn deposits

sulfide (VMS), and Archean Au-Cu porphyry deposits (e.g., Singoyi et al. 2006; Dupuis and Beaudoin 2011; Dare et al. 2014; Nadoll et al. 2014). For example, Ca+Mn+Al and Ti+V contents were used to discriminate magmatic from hydrothermal magnetite deposits (Figs. 8 and 9a) (Dupuis and Beaudoin 2011) due to extremely high Ti, Al, and V contents of magmatic magnetite (e.g., Zhou et al. 2005; Pang et al. 2008). Moreover, Ni/Cr ratios in magnetite can also be used to discriminate hydrothermal from magmatic magnetite, as the ratios for magmatic magnetite are generally <1 and for hydrothermal magnetite mostly >1 (Dare et al. 2014).

However, these discriminators above do not work well for magnetite in complex hydrothermal deposits. For example, trace element data for magnetite from skarn-type iron deposits in South China spread almost all the defined fields of the Ca+Mn+Al vs. Ti+V diagram (Hu et al. 2014; Zhao and Zhou 2015). The same problem applies to magnetite in the Fe-Cu deposits of the Kangdian Province. For example, the data for the Yinachang deposit plot in the "BIF" field of the Ca+Mn+Al vs. Ti+V diagram (Fig. 8), obviously inconsistent with our documentation of Yinachang as a hydrothermal deposit associated with extensive alteration. Thus, such discrimination plots must be used carefully in conjunction with other types of data. However, these diagrams do offer good baselines for the genetic discrimination of hydrothermal magnetite.

In order to further evaluate the possibility of using magnetite for provenance discrimination, we compare our data to those of Emeishan magmatic oxide deposits (Liu et al. 2015); the Tengtie Fe skarn deposit in SE China (Zhao and Zhou 2015); the diabase-related, hydrothermal magnetite deposits in Xinjiang Province, NW China (Huang et al. 2013b); and the Sokoman iron formation in Labrador, Canada (Chung et al. 2015). In the Ca+Mn+Al vs. Ti+V diagram (Dupuis and Beaudoin 2011), our magnetite data for the IOCG deposits in Kangdian cluster in the "BIF," "IOCG," and "Skarn" fields, whereas those of the diabase-hosted deposit in Xinjiang and the Tengtie Fe skarn deposit overlap almost completely and plot in the "Skarn" field. Also, most data of the Sokoman

iron formation do not plot in the "BIF" field (Fig. 9a). We suggest that these inconsistencies are at least partially due to poor correlation of magnetite compositions with fluid compositions.

In this study, we consider that Co, Ni, Zn, and Sn contents and their ratios can be better used for discrimination because concentrations of these elements in magnetite are thought to reflect nature of the precursor magmas producing the fluids. In a plot of Co vs. Ni, there are some overlaps of the various deposits, but it is clear that hydrothermal magnetite from the Fe-Cu deposits in the Kangdian Province plots well away from that of the Tengtie Fe skarn deposit and the Sokoman iron formation (Fig. 9b). Such a clear discrimination is genetically meaningful because Ni is generally high in magmatic fluids derived from relatively mafic magmas (Goldschmidt 1958; Carew 2004). Similarly, magnetite grains of the diabase-hosted deposits in Xinjiang and magmatic oxide deposits in Emeishan province mostly overlap with those of the Fe-Cu deposits in the Kangdian region, consistent with their precursor sources as mafic magmas. In the Zn-Sn plot, the four types of deposits cluster in different zones, but partially overlap (Fig. 9c). In the plot of Co/Ni vs. Mn, magnetite of the Kangdian Fe-Cu deposits plots well away from that of the Tengtie Fe skarn deposit without overlaps. Neither the Zn-Sn nor the Co/Ni-Mn plots can distinguish the Sokoman iron formation from Fe-Cu deposits in the Kangdian Province, but they do sufficiently discriminate magnetite in the Sokoman iron formation from those in the remaining types of deposits (Fig. 9c, d). Therefore, we suggest that these elements can potentially be used for provenance discrimination of different types of hydrothermal magnetite deposits genetically related to different magma sources.

Concluding remarks

Trace element compositions of magnetite from the Lala, Yinachang, and Dahongshan Fe-Cu deposits of the Kangdian metallogenic province, SW China, are mainly controlled by fluid compositions and/or physicochemical conditions (e.g., T and fO_2). Only influences on concentrations of V, Mo, and Sn in magnetite are partially affected by oxygen fugacity, whereas those of Cu, Zn, and Mn are partially controlled by temperature. Ore-forming fluids from which magnetite grains precipitated in the Fe-oxide stage of the Lala and Dahongshan deposits were chemically similar and are likely evolved from mafic magmas forming local, synchronous mafic intrusions. In contrast, ore-forming fluids of the Fe-oxide stage in the Yinachang deposit were compositionally different and are apparently formed from relatively oxidized, Mo-Sn-rich and evolved fluids compared to those of the Lala and Dahongshan deposits, possibly genetically related to relatively felsic magmas. Magnetite in the Cu-sulfide stage of the Lala deposit does not show large compositional differences compared to that in the Fe-oxide stage of this deposit and is thus thought to have precipitates from a common fluid evolved from the early Fe-oxide stage. On the basis of our new dataset, we also propose that the element pairs, Co vs. Ni, Zn vs. Sn, and Co/Ni vs. Mn, may be useful for provenance discrimination.

Acknowledgments We thank Paul T. Robinson for editorial improvement and Pingping Liu and Wen Zhao for sharing their compositional data of magnetite. We also appreciate the field assistance of geologists from the Lala Mine, especially Liang Chen and Dinghua Ma. Wen Zhao, Xiaowen Huang, and Ting Zhou are greatly acknowledged for their lab support. Bernd Lehmann and two anonymous reviewers are thanked for providing constructive comments. This study was supported by the National Natural Science Foundation of China (41272212), the CAS/SAFEA International Partnership Program for Creative Research Teams-Intraplate Mineralization Research Team (KZZD-EW-TZ-20), research grant of State Key Laboratory for Mineral Deposits Research (20-15-04) and a CRCG grant (201309175142).

References

Carew MJ (2004) Controls on Cu-Au mineralization and Fe oxide metasomatism in the Eastern Fold Belt, N.W. Queensland, Australia. Ph.D thesis, James Cook University, Queensland

Carranza EJM, Rondeau B, Cenki-Tok B, Fritsch E, Mazzero F, Gauthier J, Bodeur Y, Bekele E, Gaillou E, Ayalew D (2012) Geochemical characteristics of mineral deposits: implications for ore genesis. Geochem Explor Environ Anal 12:89

Chen ZL, Chen SY (1987) On the tectonic evolution of the west margin of the Yangzi Block. Chongqing Publishing House, Chongqing, p 172 (in Chinese with English abstract)

Chen WT, Zhou MF (2012) Paragenesis, stable isotopes, and molybdenite Re-Os isotope age of the Lala iron-copper deposit, Southwest China. Econ Geol 107:459–480

Chen WT, Zhou MF, Zhao XF (2013) Late Paleoproterozoic sedimentary and mafic rocks in the Hekou area, SW China: implication for the reconstruction of the Yangtze Block in Columbia. Precambrian Res 231:61–77

Chen WT, Sun WH, Wang W, Zhao JH, Zhou MF (2014a) "Grenvillian" intra-plate mafic magmatism in the southwestern Yangtze Block, SW China. Precambrian Res 242:138–153

Chen WT, Zhou MF, Gao JF (2014b) Constraints of Sr isotopic compositions of apatite and carbonates on the origin of Fe and Cu mineralizing fluids in the Lala Fe-Cu-(Mo, LREE) deposit, SW China. Ore Geol Rev 61:96–106

Chung D, Zhou MF, Gao JF, Chen WT (2015) In-situ LA-ICP-MS trace elemental analyses of magnetite: the late Palaeoproterozoic Sokoman Iron Formation in the Labrador Trough, Canada. Ore Geol Rev 65:917–928

Dare SAS, Barnes SJ, Beaudoin G (2012) Variation in trace element content of magnetite crystallized from a fractionating sulfide liquid, Sudbury, Canada: implications for provenance discrimination. Geochim Cosmochim Acta 88:27–50

Dare SAS, Barnes SJ, Beaudoin G, Meric J, Boutroy E, Potvin-Doucet C (2014) Trace elements in magnetite as petrogenetic indicators. Mineral Deposita. doi:10.1007/s00126-014-0529-0

Dupuis C, Beaudoin G (2011) Discriminant diagrams for iron oxide trace element fingerprinting of mineral deposit types. Mineral Deposita 46:319–335

Frietsch R, Perdahl JA (1995) Rare earth elements in apatite and magnetite in Kiruna-type iron ores and some other iron ore types. Ore Geol Rev 9:489–510

Gao JF, Zhou MF, Lightfoot PC, Wang CY, Qi L, Sun M (2013) Sulfide saturation and magma emplacement in the formation of the Permian Huangshandong Ni-Cu sulfide deposit, Xinjiang, northwestern China. Econ Geol 108:1833–1848

Geng Y, Yang C, Du L, Wang X, Ren L, Zhou X (2007) Chronology and tectonic environment of the Tianbaoshan Formation: new evidence from zircon SHRIMP U-Pb age and geochemistry. Geol Rev 53: 556–563 (in Chinese with English abstract)

Goldschmidt VM (1958) Geochemistry. Oxford University Press, Amen House, London

Greentree MR, Li ZX (2008) The oldest known rocks in south-western China: SHRIMP U-Pb magmatic crystallization age and detrital provenance analysis of the Paleoproterozoic Dahongshan Group. J Asian Earth Sci 33:289–302

Greentree MR, Li ZX, Li XH, Wu HC (2006) Late Mesoproterozoic to earliest Neoproterozoic basin record of the Sibao orogenesis in western South China and relationship to the assembly of Rodinia. Precambrian Res 151:79–100

Guo Y, Wang S, Sun X, Liao Z, Wang Z, Zhou B, Yang B (2014) Zircon U-Pb age of the Paleoproterozoic diabase from the Yinachang iron-copper deposit, Yunnan Province, and its geological implication. Geotecton Metallog 38:208–215 (in Chinese with English abstract)

He J (1980) The albite metasomatites and their original rocks, Lala, Huili, western Sichuan. Bull Chengdu Inst Geol Min Res, Chinese Acad Geol Sci 1:60–79 (in Chinese with English abstract)

Hou L, Ding J, Wang CM, Liao ZW, Guo Y, Wang SW, Wang ZZ (2013) Ore-forming fluid and metallogenesis of the Yinachang Fe-Cu-Au-REE deposit, Wuding, Yunnan Province, China. Acta Petrol Sin 29(4):1187–1202 (in Chinese with English abstract)

Hou L, Ding J, Deng J, Peng HJ (2014) Geology, geochronology, and geochemistry of the Yinachang Fe-Cu-Au-REE deposit of the Kangdian region of SW China: evidence for a Paleo-Mesoproterozoic tectono-magmatic event and associated IOCG systems in the western Yangtze Block. J Asian Earth Sci. doi:10.1016/j.jseaes.2014.09.016

Hu H, Li JW, Lentz D, Ren Z, Zhao XF, Deng XD, Hall D (2014) Dissolution-reprecipitation process of magnetite from the Chengchao iron deposit: insights into ore genesis and implication for in-situ chemical analysis of magnetite. Ore Geol Rev 57: 393–405

Huang XW, Zhao XF, Qi L, Zhou MF (2013a) Re-Os and S isotopic constraints on the origins of two mineralization events at the Tangdan sedimentary rock-hosted stratiform Cu-deposit, SW China. Chem Geol 347:9–19

Huang XW, Zhou MF, Qi L, Gao JF, Wang YW (2013b) Re-Os isotopic ages of pyrite and chemical composition of magnetite from the Cihai magmatic-hydrothermal Fe deposit, NW China. Mineral Deposita 48:925–946

Ilton ES, Eugster HP (1989) Base metal exchange between magnetite and chloride-rich hydrothermal fluid. Geochim Cosmochim Acta 53: 291–301

Jin MX, Shen S (1998) Fluid features and metallogenic conditions in Lala copper deposit, Huili, Sichuan, China. Geol Sci Technol Inf 17:45–48 (in Chinese with English abstract)

Li ZQ, Hu RZ, Wang JZ, Liu JJ, Li CY, Liu YP, Ye L (2002) Lala Fe-oxide-Cu-Au-U-REE ore deposit, Sichuan China: an example of superimposed mineralization. Bull Mineral Petrol Geochem 21: 258–260 (in Chinese with English abstract)

Li ZQ, Wang JZ, Liu JJ, Li CY, Du AD, Liu YP, Ye L (2003a) Re-Os dating of molybdenite from Lala Fe-oxide-Cu-Au-Mo-REE deposit, southwest China: implications for ore genesis. Contrib Geol Min Resour Res 18:39–42, in Chinese with English abstract

Li ZX, Li XH, Kinny PD, Wang J, Zhang S, Zhou H (2003b) Geochronology of Neoproterozoic syn-rift magmatism in the Yangtze Craton, South China and correlations with other continents: evidence for a mantle superplume that broke up Rodinia. Precambrian Res 122:85–109

Liu YS, Hu ZC, Gao S, Gunther D, Xu J, Gao CG, Chen HH (2008) In situ analysis of major and trace elements of anhydrous minerals by LA-ICP-MS without applying an internal standard. Chem Geol 257: 34–43

Liu PP, Zhou MF, Chen WT, Gao JF, Huang XW (2015) In-situ LA-ICP-MS trace elemental analyses of magnetite: Fe-Ti-(V) oxide-bearing mafic-ultramafic layered intrusions of the Emeishan Large igneous Province, SW China. Ore Geol Rev 65:853–871

Müller B, Axelsson MD, Ohlander B (2003) Trace elements in magnetite from Kiruna, northern Sweden, as determined by LA-ICP-MS. GFF 125:1–5

Nadoll P, Koenig AE (2011) LA-ICP-MS of magnetite: methods and reference materials. J Anal At Spectrom 26:1872–1877

Nadoll P, Angerer T, Mauk JL, French D, Walshe J (2014) The chemistry of hydrothermal magnetite: a review. Ore Geol Rev 61:1–32

Neilson R (2003) Trace element partitioning, http://earthref.org/GERM/tolls/tep.htm

Nystrom JO, Henriquez F (1994) Magmatic features of iron ores of the Kiruna type in Chile and Sweden: ore textures and magnetite geochemistry. Econ Geol 89:820–839

Pearce JA, Gale G (1977) Identification of ore-deposition environment from trace-element geochemistry of associated igneous host rocks. Geol Soc Lond, Spec Publ 7:14–24

Qian J, Shen Y (1990) The Dahongshan volcanogenic Fe-Cu deposit in Yunnan Province: series of geological memoirs of People's Republic of China. Geological Publishing House, Beijing, p 236 (in Chinese with English abstract)

Pang KN, Zhou MF, Lindsley D, Zhao DG, Malpas J (2008) Origin of Fe-Ti oxides ores in mafic intrusions: evidence from the Panzhihua intrusion, SW China. Journal of Petrology 49: 295–313

Shentu BY (1997) Geological and geochemical characteristics of the Lala copper deposit and its formation model. Tethyan Geol 21:112–126 (in Chinese)

Singoyi B, Danyushevsky L, Davidson GJ, Large R, Zaw K (2006) Determination of trace elements in magnetites from hydrothermal deposits using the LA-ICP-MS technique. Abstracts of Oral and Poster Presentations from the SEG 2006 Conference Society of Economic Geologists, Keystone, USA 367–368

Sun K, Shen Y, Liu G, Li Z, Pan X (1991) Proterozoic iron-copper deposits in central Yunnan Province. China University of Geoscience Press, Wuhan, p 169 (in Chinese with English abstract)

Sun Y, Shu XL, Xiao YF (2006) Isotopic geochemistry of the Lala copper deposit, Sichuan Province, China and its metallogenetic significance. Geochimica 35:553–559 (in Chinese with English abstract)

Sun WH, Zhou MF, Gao JF, Yang YH, Zhao XF, Zhao JH (2009) Detrital zircon U-Pb geochronological and Lu-Hf isotopic constraints on the Precambrian magmatic and crustal evolution of the western Yangtze Block, SW China. Precambrian Res 172:99–126

Toplis ML, Corgne A (2002) An experimental study of element partitioning between magnetite, clinopyroxene and iron-bearing silicate liquids with particular emphasis on vanadium. Contrib Mineral Petrol 144:22–37

Wang W, Zhou MF (2014) Provenance and tectonic setting of the Paleo- to Mesoproterozoic Dongchuan Group in the southwestern Yangtze Block, South China: implication for the breakup of the supercontinent Columbia. Tectonophysics 610:110–127

Wang ZZ, Zhou BG, Guo Y, Yang B, Liao ZW, Wang SW (2012) Geochemistry and zircon U-Pb dating of Tangtang granite in the western margin of the Yangtze Platform. Acta Petrol Mineral 31: 652–662 (in Chinese with English abstract)

White WH, Bookstrom AA, Kamilli RJ, Ganster MW, Smith RP, Ranta DE, Steninger RC (1981) Character and origin of climax-type molybdenum deposits. In: Skinner BJ (ed.), Economic geology 75th Anniversary Volume: 270–316

Wu MD, Duan JS, Song XL, Chen LZ, Dan YQ (1990) Geology of Kunyang Group in Yunnan. Yunnan Science and Technology Press, Kunming, p 265 (in Chinese)

Ye XT, Zhu WG, Zhong H, He DF, Ren T, Bai ZJ, Fan HP, Hu WJ (2013) Zircon U-Pb and chalcopyrite Re-Os geochronology, REE geochemistry of the Yinachang Fe-Cu-REE deposit in Yunnan Province and its geological significance. Acta Petrol Sin 29(4):1167–1186 (in Chinese with English abstract)

Zhao XF (2010) Paleoproterozoic crustal evolution and Fe-Cu metallogeny of the western Yangtze Block, SW China. Unpublished Ph.D thesis, Hong Kong, China, The University of Hong Kong, pp 53–55

Zhao XF, Zhou MF (2011) Fe-Cu deposits in the Kangdian region, SW China: a Proterozoic IOCG (iron-oxide-copper-gold) metallogenic province. Mineral Deposita 46:731–747

Zhao WW, Zhou MF (2015) In-situ LA-ICP-MS trace elemental analyses of magnetite: the Mesozoic Tengtie skarn Fe deposit in the Nanling Range, South China. Ore Geol Rev 65:872–883

Zhao XF, Zhou MF, Li JW, Sun M, Gao JF, Sun WH, Yang JH (2010) Late Paleoproterozoic to early Mesoproterozoic Dongchuan Group in Yunnan, SW China: implications for tectonic evolution of the Yangtze Block. Precambrian Res 182:57–69

Zhao XF, Zhou MF, Li JW, Seley D, Li XH, Qi L (2013) Sulfide Re-Os and Rb-Sr isotope dating of the Kangdian IOCG metallogenic province, southwest China: implications for regional metallogenesis. Econ Geol 108:1489–1498

Zhou MF, Yan DP, Kennedy AK, Li Y, Ding J (2002) SHRIMP U-Pb zircon geochronological and geochemical evidence for Neoproterozoic arc-magmatism along the western margin of the Yangtze Block, South China. Earth Planet Sci Lett 196:51–67

Zhou MF, Robinson PT, Lesher CM, Keays RR, Zhang CJ, Malpas J (2005) Geochemistry, petrogenesis and metallogenesis of the Panzhihua Gabbroic Layered Intrusion and associated Fe-Ti-V oxide deposits, Sichuan Province, SW China. Journal of Petrology 46: 2253–2280

Zhou MF, Ma Y, Yan DP, Xia X, Zhao JH, Sun M (2006) The Yanbian Terrane (Southern Sichuan Province, SW China): a Neoproterozoic arc assemblage in the western margin of the Yangtze Block. Precambrian Res 144:19–38

Zhou MF, Zhao XF, Chen WT, Li XC, Wang W, Yan DP, Qiu HN (2014) Proterozoic Fe-Cu metallogeny and supercontinental cycles of the southwestern Yangtze Block, southern China and northern Vietnam. Earth-Science Reviews 139: 59–82

Zhu ZM (2011) Lala iron oxide copper gold deposit: metallogenic epoch and metal sources. Ph.D thesis, Chengdu, China, Chengdu University of Technology, pp 52–54

Zhu ZM, Zeng LX, Zhou JY, Luo LP, Chen JB, Shen B (2009) Lala iron oxide-copper-gold deposit in Sichuan Province: evidence from mineralography. Geol J China Univ 15:485–495 (in Chinese with English abstract)